Solution and Solid-State Characteristics of Imine Adducts with Tris(pentafluorophenyl)borane

James M. Blackwell,[†] Warren E. Piers,*[,†,1] Masood Parvez,[†] and Robert McDonald[‡]

Department of Chemistry, University of Calgary, 2500 University Drive NW, Calgary, Alberta T2N 1N4, Canada, and X-ray Structure Laboratory, Department of Chemistry, University of Alberta, Edmonton, Alberta T6G 2G2, Canada

Received December 21, 2001

Adducts of the *N*-benzyl imines Ph(R)C═NBn (R = Ph, CH_3, H) and ^{t}Bu(CH_3)C═NBn and the *N*-phenyl imine Ph(H)C═NPh with the Lewis acid tris(pentafluorophenyl)borane, $B(C_6F_5)_3$, have been prepared and characterized in solution and in the solid state. For each imine, the Lewis acid is N-bound, with the exception of the sterically demanding base ^{t}Bu(CH_3)C═NBn, which reacts with $B(C_6F_5)_3$ through its enamine tautomer to form an α-C bound adduct, **5**. In the N-bound imine−borane adducts **1**−**4**, steric crowding and π-stacking between C_6F_5 and C_6H_5 rings results in restricted rotation about the B−N and B−C bonds; the dynamic behavior which results can be studied using variable-temperature ^{19}F and ^{1}H NMR spectroscopy. For the unsymmetrical ketimines and aldimines, kinetic adducts of the thermodynamically dominant free imine are observed to form initially upon treatment with $B(C_6F_5)_3$; these adducts slowly convert thermally to the thermodynamic adducts of the less stable imine. For the ketimine Ph(CH_3)C═NBn, both the kinetic adduct **2-k** and the thermodynamic adduct **2-t** were fully characterized. In the solid-state structures of all the adducts except **5**, one or two C_6F_5/C_6H_5 stacking interactions are present; in one case, the adduct **3-t** between $B(C_6F_5)_3$ and Ph(H)C═NBn, intermolecular stacking interactions are apparent in the crystal-packing diagram. The implications of the structures of these adducts for Lewis acid mediated addition of nucleophiles to imines is discussed.

Introduction

The addition of nucleophiles to imines is an important transformation in organic synthesis.[2] Although addition of strong nucleophiles can occur without external activation, weaker addends are often assisted by a Lewis acid, either in stoichiometric amounts or in catalytic quantities.[3] Even with strong nucleophiles, use of a Lewis acid can be advantageous in order to modulate the reactivity or control the stereoselectivity. The role of the Lewis acid in these reactions is mostly thought to involve further polarization of the C═N bond via coordination of the Lewis acid to the imine nitrogen lone pair, although few detailed mechanistic studies probing this question have been reported.[4]

It is widely acknowledged that the possibility exists for geometrical isomers (syn vs anti) of imine adducts of Lewis acids (eq 1). Although it has often been

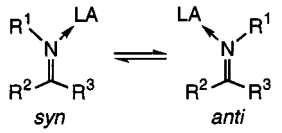

(1)

hypothesized that competitive reaction via these isomers can affect the stereochemical outcome of addition to the imine, there are few studies which experimentally demonstrate that such syn−anti isomerism is an important factor to consider.[5] The most striking recent example is the enantioselective reduction of imines, as mediated by titanocene catalysts reported by Buchwald et al.[6] In this chemistry, the enantioselectivity can be modulated by reducing the H_2 pressure and allowing for syn−anti isomerization to become kinetically competitive with hydrogenation.

Despite the importance of Lewis acid/imine adducts in this arena, few studies concerning the solution and

* To whom correspondence should be addressed. Phone: 403-220-5746. Fax: 403-289-9488. E-mail: wpiers@ucalgary.ca.
† University of Calgary.
‡ University of Alberta.
(1) S. Robert Blair Professor of Chemistry 2000−2005. NSERC E. W. R. Steacie Fellow 2001−2003.
(2) Larock, R. C. *Comprehensive Organic Transformations*, 2nd ed.; Wiley-VCH: New York, 1999; pp 835−866.
(3) (a) Denmark, S. E.; Nicaise, O. J.-C. In *Comprehensive Asymmetric Catalysis*; Jacobsen, E. N., Pfaltz, A., Yamamoto, H., Eds.; Springer-Verlag: New York, 1999; Vol. 2, pp 923−964. (b) Bloch, R. *Chem. Rev.* **1998**, *98*, 1407. (c) Enders, D.; Reinhold, U. *Tetrahedron: Asymmetry* **1997**, *8*, 1895.
(4) Aubrecht, K. B.; Winemillar, M. D.; Collum, D. B. *J. Am. Chem. Soc.* **2000**, *122*, 11084.
(5) (a) Keck, G. E.; Enholdm, E. J. *J. Org. Chem.* **1985**, *50*, 146. (b) Shimizu, M.; Kume, K.; Fujisawa, T. *Tetrahedron Lett.* **1982**, *23*, 3739. (c) Chen, C.-M.; Brown, H. C. *J. Am. Chem. Soc.* **2000**, *122*, 4217.
(6) Willoughby, C. A.; Buchwald, S. L. *J. Am. Chem. Soc.* **1994**, *116*, 8952.

10.1021/om011086n CCC: $22.00
Publication on Web 02/28/2002

Scheme 1

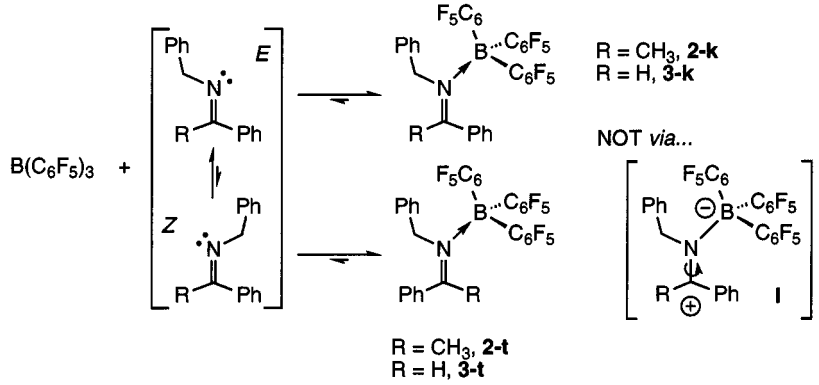

solid-state structures of the adducts between monodentate imines and main-group Lewis acids have been undertaken.[7] Our interest in addition reactions to carbonyl[8] and imine[9] functions as catalyzed by the strong organometallic Lewis acid $B(C_6F_5)_3$[10−12] has led us to explore the stoichiometric reactivity of this borane with simple aldimines and ketimines. Due to the high stability and strength of this Lewis acid, adducts with a variety of weak Lewis bases have been readily generated and studied both in solution and in the solid state.[13] Herein we describe stoichiometric reactions between $B(C_6F_5)_3$ and four *N*-benzyl imines and one *N*-phenyl imine and the solution and solid-state characteristics of the resulting adducts. The nature of the thermodynamic products of these complexations is dependent on the features of the imine, and the results have implications for the role of the Lewis acid in the promoted reactions of imines with nucleophiles.

Results and Discussion

Solution Structure and Dynamics of $B(C_6F_5)_3$−Imine Adducts. The symmetrical *N*-benzyl ketimine $Ph_2C{=}NBn$ forms an adduct with $B(C_6F_5)_3$, **1**, (eq 2), which exhibits a rigid structure in solution, as evidenced by the observation of 15 separate signals for the aryl fluoro groups in the ^{19}F NMR spectrum at room temperature. The absence of exchange both between and

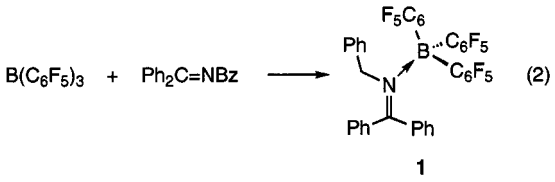

within the C_6F_5 rings suggests that rotation about the B−N vector and the B−C bonds is restricted in this congested adduct. Heating the sample to 60 °C results in severe broadening in the spectrum, indicating that some freedom to rotate exists. In the ^1H NMR spectrum, the benzylic protons are diastereotopic in the static structure but are observed to coalesce at about 40 °C, corresponding to a barrier of $\Delta G^{\ddagger} = 59.9(5)$ kJ mol^{-1} for the exchange of these two protons.

For unsymmetrical ketimines or aldimines, the situation is somewhat more complex. In these systems, a kinetic adduct is observed initially, followed by slow emergence of a thermodynamic adduct (Scheme 1) over the course of about 1 h. For example, for the reaction between $B(C_6F_5)_3$ and the ketimine $Ph(CH_3)C{=}NBn$ (which exists in solution as a 17:1 equilibrium mixture of the *E* and *Z* isomers[6]) at −40 °C, the initial adduct **2-k** is observed by both ^1H and ^{19}F NMR spectroscopy. When the temperature is raised, a new adduct, **2-t**, appears, eventually supplanting the kinetic adduct such that the final ratio is approximately 10:1 in toluene. In C_6D_6, where the final ratio of **2-t** to **2-k** is 5:1, 1-D NOE experiments support the assignment of the kinetic adduct as the isomer with the borane syn to the imine phenyl group. For example, irradiation of the N-benzylic protons in **2-k** results in NOE enhancement of the methyl protons; such an enhancement is not observed in **2-t**. Furthermore, in a $^{19}F/^1H$ NOE experiment, irradiation of the *o*-fluorine resonances in **2-t** results in a positive enhancement of the ketimine methyl protons which is absent in the kinetic structure. As indicated in Scheme 1, similar results are obtained for the aldimine $Ph(H)C{=}NBn$, where the products **3-k** and **3-t** are observed to form.

The process by which this isomerization of adducts occurs is likely via the free imines, rather than a Lewis acid activated structure akin to **I** depicted in Scheme

(7) Of course, many examples of transition-metal and main-group complexes that incorporate ligands in which an imine function is part of a chelate array exist; we do not include this class of compounds in this statement.

(8) (a) Parks, D. J.; Piers, W. E. *J. Am. Chem. Soc.* **1996**, *118*, 9440. (b) Parks, D. J.; Blackwell, J. M.; Piers, W. E. *J. Org. Chem.* **2000**, *65*, 3090. (c) Blackwell, J. M.; Piers, W. E. *Org. Lett.* **2000**, *2*, 695. (d) Blackwell, J. M.; Piers, W. E.; McDonald, R. *J. Am. Chem. Soc.* **2002**, *124*, 1295.

(9) Blackwell, J. M.; Sonmor, E.; Scoccitti, T.; Piers, W. E. *Org. Lett.* **2000**, *2*, 3921.

(10) (a) Massey, A. G.; Park, A. J.; Stone, F. G. A. *Proc. Chem. Soc.* **1963**, 212. (b) Massey, A. G.; Park, A. J. *J. Organomet. Chem.* **1964**, *2*, 245.

(11) For reviews on the use of this Lewis acid in organic synthesis see: (a) Piers, W. E.; Chivers, T. *Chem. Soc. Rev.* **1997**, 345. (b) Ishihara, K.; Yamamoto, *Eur. J. Org. Chem.* **1999**, *527*, 7. For a review on its use in organometallic chemistry see: Chen, E. Y.-X.; Marks, T. J. *Chem. Rev.* **2000**, *100*, 1391.

(12) Recent examples of the use of $B(C_6F_5)_3$ as a Lewis acid in organic transformations: (a) Blackwell, J. M.; Foster, K. L.; Beck, V. H.; Piers, W. E. *J. Org. Chem.* **1999**, *64*, 4887. (b) Hassfield, J.; Christmann, M.; Kalesse, M. *Org. Lett.* **2001**, *3*, 3561. (c) Gevorgyan, V.; Liu, J.-X.; Rubin, M.; Benson, S.; Yamamoto, Y. *Tetrahedron Lett.* **1999**, *40*, 8919. (d) Gevorgyan, V.; Rubin, M.; Benson, S.; Liu, J.-X.; Yamamoto, Y. *J. Org. Chem.* **2000**, *65*, 6179. (e) Rubin, M.; Gevorgyan, V. *Org. Lett.* **2001**, *3*, 2705. (f) Imamura, K.; Yoshikawa, E.; Gevorgyan, V.; Sudo, T.; Asao, N.; Yamamoto, Y. *Can. J. Chem.* **2001**, *79*, 1624.

(13) (a) Röttger, D.; Erker, G.; Fröhlich, R.; Kotila, S. *J. Organomet. Chem.* **1996**, *518*, 17. (b) Bradley, D. C.; Hursthouse, M. B.; Motevalli, M.; Zheng, D. H. *J. Chem. Soc., Chem. Commun.* **1991**, 7. (c) Bradley, D. C.; Harding, I. S.; Keefe, A. D.; Motevalli, M.; Zheng, D. H. *J. Chem. Soc., Dalton Trans.* **1996**, 3931. (d) Parks, D. J.; Piers, W. E.; Parvez, M.; Atencio, R.; Zaworotko, M. J. *Organometallics* **1998**, *17*, 1369.

1.[14] This is supported by the observation that, in the presence of an excess of borane, the isomerization of **2-k** to **2-t** or of **3k** to **3t** is significantly inhibited. The rate-limiting step in the adduct isomerization is likely the thermal isomerization of the free imine rather than the dissociative step necessary to produce free imine. At room temperature, the adducts are kinetically labile, as demonstrated by the facile dissociative substitution of less basic imines (e.g. $Ph_2C{=}NBn$) with more basic bonding partners (e.g. $Ph(CH_3)C{=}NBn$). These equilibria are established essentially upon mixing. On the other hand, first-order rate constants for the thermal *E*/*Z* isomerization of N-alkyl-substituted imines (which occurs via inversion at the imine N) yield half-lives on the order of a few hours for this process,[15] the same time scale as the observed equilibration of **2-k/3-k** to **2-t/3-t**. Thus, upon mixing, the borane reacts rapidly with the thermodynamically prevalent free imine to give the more sterically hindered adduct but gradually converts to the thermodynamically more favored adduct by trapping the less stable *Z* isomer of the imine.

Spectroscopically, the kinetic adducts **2-k** and **3-k**, where $B(C_6F_5)_3$ is found syn to the imine phenyl group, behave very similarly to adduct **1**, where the borane has no choice but to be syn to a phenyl group. In the ^{19}F NMR spectra of these adducts, 15 separate signals are again observed, and coalescence behavior in the benzylic protons is found in the ^1H NMR spectra, with a barrier for this exchange of $\Delta G^{\ddagger} = 58.5(5)$ kJ mol^{-1} at 20 °C estimated for kinetic adduct **3-k**. A measurement of the analogous barrier for **2-k** could not be made, since the diastereotopic benzylic protons in **2-k** have nearly coincident chemical shifts. The barrier in **3-t**, where borane is syn to the aldimine proton, is somewhat lower ($\Delta G^{\ddagger} = 52.1(5)$ kJ mol^{-1} at −10 °C). Nonetheless, in both **2-t** ($\Delta G^{\ddagger} = 66.6(5)$ kJ mol^{-1} at 56 °C) and **3-t**, restricted rotation in the B−N and B−C bonds is observed, resulting in diastereotopic benzylic protons and C_6F_5 rings and attesting to the steric crowding inherent even in the thermodynamic structures of these adducts.

To probe the nature and strength of C_6F_5/C_6H_5 π-stacking interactions in these adducts (see below), the reactions of two further imines with $B(C_6F_5)_3$ were studied. For *N*-benzylideneaniline ($Ph(H)C{=}NPh$), in which the N−Bn group is replaces with an N−Ph substitutent, solution chemistry very similar to that described above was observed. However, in this instance, only the thermodynamic isomer of the adduct, **4-t**, was fully characterized. The last imine studied was

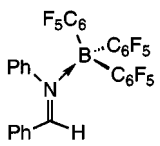

4-t

the aliphatic ketimine $^tBu(CH_3)C{=}NBn$, which undergoes an unexpected reaction with $B(C_6F_5)_3$. Upon addition of 1 equiv of borane to $^tBu(CH_3)C{=}NBn$, approximately 40% of the imine is converted to a new compound for which the NMR spectral data is in disaccord with those expected for either kinetic or thermodynamic N-bound adducts analogous to those described above. This new product predominates in solution when 3 equiv more of $B(C_6F_5)_3$ is added. In the ^{19}F NMR spectrum of this mixture, in addition to signals for free borane, three new signals are observed, suggesting that free rotation of the C_6F_5 moieties is possible in this species. The ^{11}B NMR spectrum shows a resonance at −12.2 ppm, about 10 ppm upfield of the resonances typically observed for adducts **1**−**4** and indicative of a borate-type boron rather than a neutral, four-coordinate center. The ^1H NMR spectrum shows three nonaromatic signals in a 2:2:9 ratio rather than the 2:3:9 ratio observed for the free ketimine. Finally, the ^{13}C NMR spectrum shows four nonaromatic signals, including one at 212.8 ppm for the imine C=N carbon. This resonance is shifted significantly downfield relative to that observed for the free imine (175.1 ppm) in C_6D_6. These data are consistent with the formation of the iminium zwitterion **5**, as shown in eq 3. This species presumably forms because

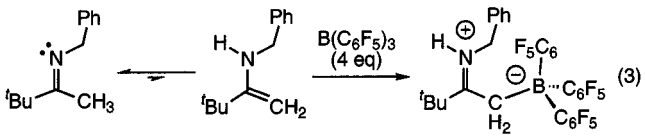

5

steric effects destabilize borane binding to the imine nitrogen. The sterically demanding ^{t}Bu group cannot accommodate either the borane or the benzyl group in a syn orientation. Thus, the borane traps the imine as its enamine tautomer, forming **5**.

This assignment was confirmed by X-ray crystallography; an ORTEP diagram of **5** is given in Figure 1, along with selected bond distances and angles. The metrical data are supportive of the zwitterionic resonance form, although the C(1)−N(1) bond length of 1.3024(18) Å is slightly longer than the typical C=N distance of 1.28 Å and the C(1)−C(2) separation of 1.4750(19) Å is somewhat shorter than that expected for an sp^2-sp^3 C−C bond (~1.50 Å). Also, the B−C(2) distance of 1.715(2) Å is rather long in comparison to the other B−C bonds in the structure and also to the B−C bond length of 1.675(2) Å in the related adduct $B(C_6F_5)_3{\cdot}CH_2PPh_3$.[16] These data are thus consistent with the observation that, in solution, this is a weak adduct whose formation must be driven by the presence of excess Lewis acid. To our knowledge, this type of reactivity between an imine and a Lewis acid has not been observed or given much consideration previously.

Solid State Structures of N−Bound Imine Adducts. The adducts **1**−**4** are all white crystalline solids which can be isolated analytically pure in 50−90% yield after one recrystallization. Thus, it was possible to analyze the adducts **1**, **2-k**, **2-t**, **3-t**, and **4-t** by X-ray crystallography. Comparative metrical data are given in Table 1; for **2-k**, two independent molecules with similar parameters were refined. In general, the in-

(14) Acid-catalyzed isomerizations of imines generally occur only in the presence of a nucleophile (usually the counteranion of the acid moiety): Johnson, J. E.; Morales, N. M.; Gorczyca, A. M.; Dolliver, D. D.; McAllister, M. A. *J. Org. Chem.* **2001**, *66*, 7979 and references therein.

(15) McCarty, C. G. In *The Chemistry of the Carbon-Nitrogen Double Bond*; Patai, S., Ed.; Wiley-Interscience: Toronto, 1970; p 363.

(16) Döring, S.; Erker, G.; Fröhlich, R.; Meyer, O.; Bergander, K. *Organometallics* **1998**, *17*, 2183.

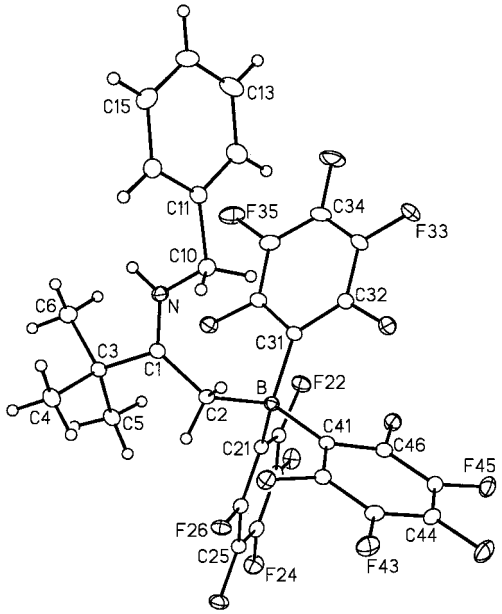

Figure 1. ORTEP diagram of **5**. Selected bond distances (Å): N−C(1), 1.305(2); C(1)−C(2), 1.475(2); B−C(2), 1.715(2); B−C(21), 1.665(2); B−C(31), 1.657(2); B−C(41), 1.667(2); N−C(10), 1.489(2). Selected bond angles (deg): C(10)−N−C(1), 126.7(1); N−C(1)−C(2), 119.5(1); N−C(1)−C(3), 117.2(1); C(3)−C(1)−C(2), 112.7(1); C(1)−C(2)−B, 121.6(1).

Table 1. Metrical Parameters for N-Bound $B(C_6F_5)_3$−Imine Adducts

adduct	C=N (Å)	N−B (Å)	N−C_{Bn} (Å)	C=N−C_{Bn} (deg)	C=N−B (deg)	C_{Bn}−N−B (deg)
1	1.297(6)	1.642(8)	1.502(6)	117.0(4)	133.2(5)	109.6(4)
2-k						
a	1.300(5)	1.630(6)	1.504(5)	116.8(4)	132.2(4)	110.6(3)
b	1.310(5)	1.658(6)	1.498(5)	118.0(4)	132.2(4)	109.5(4)
2-t	1.293(2)	1.640(2)	1.502(2)	118.1(1)	131.2(2)	110.5(1)
3-t	1.285(2)	1.627(3)	1.481(2)	121.1(2)	124.6(2)	114.3(1)
4-t[a]	1.296(4)	1.649(4)	1.454(4)	118.4(6)	119.6(3)	121.8(2)

[a] C_{Bn} in this compound is C_{ipso} of the *N*-phenyl group.

tramolecular metrical data are similar in these adducts. The C=N distances are only slightly elongated from the expected value of ∼1.28 Å for a "normal" C=N bond; B−N distances are somewhat longer than those found in $B(C_6F_5)_3$−nitrile adducts (1.595(3)−1.616(3) Å[17]), as expected on the basis of the higher steric requirements of imine Lewis bases. The angles about N can be rationalized by consideration of the steric properties of the group syn to the borane.

Perhaps more interesting are the nonbonding interactions present in these molecules, in the form of π-stacking interactions between $-C_6F_5$ and $-C_6H_5$ moieties. We have previously noted such an interaction in the solid-state structures of the adducts between $B(C_6F_5)_3$ and PhC(O)R (R = OEt, N^iPr_2) and, through low-temperature NMR spectroscopy, demonstrated their importance in solution structures as well.[13d] The ability of these two groups to stack relates to their oppositely charged quadrupoles; perfluorinated rings are electron poor above the aromatic plane, whereas protioaryl rings are electron rich. The strength of the interaction is not great; estimates of about 15.5 kJ mol^{-1} for the C_6F_6/C_6H_6 pair have been measured,[18] while other studies suggest that each fluorine contributes about 2.5 kJ mol^{-1} to the interaction strength.[19] Nonetheless, these weakly energetic interactions can have remarkable effects on subsequent chemistry,[20] and in the present study, the stereochemical rigidity observed in solution for several of these adducts can be at least partially rationalized in terms of the intramolecular stacking interactions.

Table 2. Distances (Å) between Stacked C_6F_5 and *N*-Benzyl C_6H_5 Rings

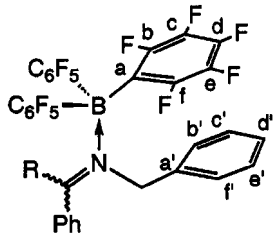

position	**1**	**2-k**(a)	**2-k**(b)	**2-t**	**3-t**
a/a′	3.052	3.123	3.092	3.121	3.062
b/b′	3.338	3.503	3.476	3.392	3.119
c/c′	3.829	3.905	3.945	3.769	3.454
d/d′	3.992	3.997	4.018	3.935	3.710
e/e′	3.691	3.652	3.621	3.686	3.655
f/f′	3.212	3.219	3.178	3.237	3.336
av	3.519	3.567	3.555	3.523	3.389

Two different intramolecular π-stacking interactions are found in this family of compounds. One exists between the phenyl group of the benzyl moiety and a borane C_6F_5 ring, while the other is between the syn iminyl phenyl group and is similar in character to those found in the $B(C_6F_5)_3$·PhC(O)R adducts mentioned above.[13d] Table 2 collects the intrastack distances for the *N*-benzyl/C_6F_5 interaction in these imine adducts, while Table 3 lists those for the iminyl phenyl/C_6F_5 stacks. The average separation between the ring atoms found in all cases are well within observed distances for other π-stacked complexes.[13d,20]

Adducts **1** and **2-k**, where the borane is coordinated syn to an iminyl phenyl group, feature both of these stacking interactions. Figures 2 and 3 show views of **1** and **2-k**, respectively, which emphasize the two interactions. In general, the average values for the intrastack distances of the aromatic carbons are slightly smaller for the benzyl/C_6F_5 interaction than the iminyl phenyl/C_6F_5 stack but both interactions are geometrically very similar, being separated by the same number of atoms. In the adducts **2-t** and **3-t**, where the borane is now coordinated anti to the iminyl phenyl group, this stacking interaction is lost and only that with the N-benzyl group is possible. Figure 4 shows a view of **2-t** which illustrates the presence of only one intramolecular stacking interaction with the N−Bn group. Interest-

(17) Jacobsen, H.; Berke, H.; Döring, S.; Kehr, G.; Erker, G.; Fröhlich, R.; Meyer, O. *Organometallics* **1999**, *18*, 1724,

(18) Williams, J. H. *Acc. Chem. Res.* **1993**, *26*, 593.

(19) Cozzi, F.; Ponzini, F.; Annunziata, R.; Cinquinei, M.; Siegel, J. S. *Angew. Chem., Int. Ed. Engl.* **1995**, *34*, 1019.

(20) (a) Coates, G. W.; Waymouth, R. M. *Science* **1995**, *267*, 217. (b) Pietsch, M. A.; Rappe, A. K. *J. Am. Chem. Soc.* **1996**, *118*, 10908. (c) Coates, G. W.; Dunn, A. R.; Henling, L. M.; Dougherty, D. A.; Grubbs, R. H. *Angew. Chem., Int. Ed. Engl.* **1997**, *36*, 248. (d) Coates, G. W.; Dunn, A. R.; Henling, L. M.; Ziller, J. W.; Lobkovsky, E. B.; Grubbs, R. H. *J. Am. Chem. Soc.* **1998**, *120*, 3641. (e) Weck, M.; Dunn, A. R.; Matsumoto, K.; Coates, G. W.; Lobkovsky, E. B.; Grubbs, R. H. *Angew. Chem., Int. Ed.* **1999**, *38*, 2741. (f) Dai, C.; Nguyen, P.; Marder, T. B.; Scott, A. J.; Clegg, W.; Viney, C. *Chem. Commun.* **1999**, 2493.

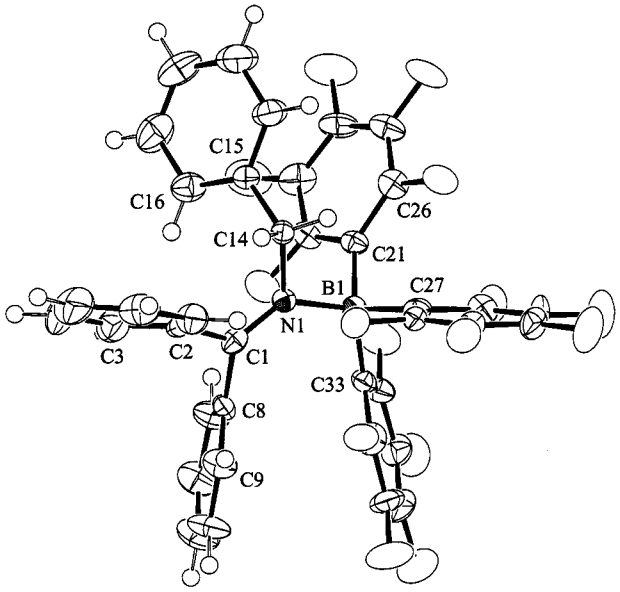

Figure 2. ORTEP diagram of **1**. See Tables 1−3 for selected metrical parameters.

Table 3. Distances (Å) between Stacked C_6F_5 and Iminyl C_6H_5 Rings

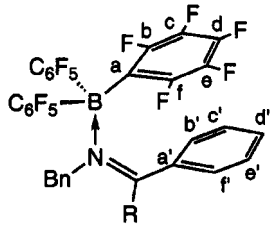

position	**1**	**2-k**(a)	**2-k**(b)
a/a′	3.084	3.062	3.017
b/b′	3.579	3.534	3.445
c/c′	4.176	4.121	3.887
d/d′	4.243	4.224	3.901
e/e′	3.795	3.756	3.543
f/f′	3.313	3.258	3.173
av	3.698	3.659	3.494

ingly, however, for aldimine adduct **3-t**, which crystallizes in a different space group than ketimine adduct **2-t**, *inter*molecular stacking interactions are observed. While only one intramolecular stack is possible (Figure 5a), the molecules line up in the crystal such that an alternating arrangement of benzylic C_6H_5 and $B-C_6F_5$ rings are made possible (Figure 5b). The intermolecular distances between the rings range from 3.34 to 3.967 Å, which are again well within the distances expected for stacked rings. This motif is absent in the packing structures of all the other adducts described herein, including the closely related adduct **2-t**, which differs only in the presence of a methyl group on the imine carbon rather than hydrogen. Finally, the structure of the adduct with the *N*-phenyl-substituted imine, **4-t**, reveals that a stacking interaction with this group is geometrically more difficult (Figure 6) due to the difficulty in attaining an eclipsed geometry. As a result, the average inter-ring distance of 4.23 Å is somewhat larger for this species compared to those discussed above.

It is possible that these π-stacking interactions may contribute to the barriers observed for exchange of the

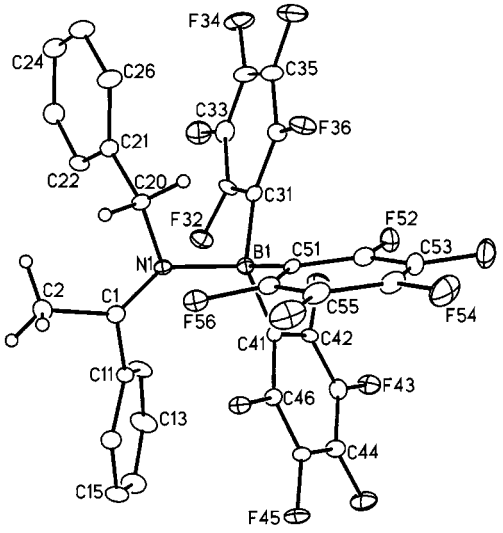

Figure 3. ORTEP diagram of **2-k** (molecule A). See Tables 1−3 for selected metrical parameters.

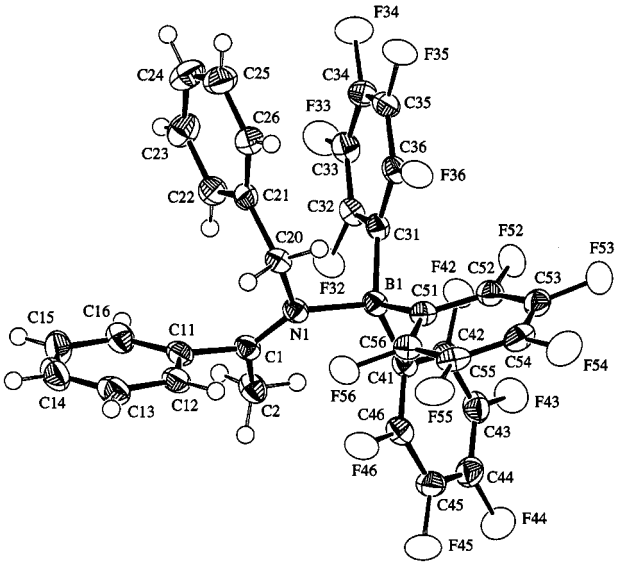

Figure 4. ORTEP diagram of **2-t**. See Tables 1−3 for selected metrical parameters.

$-C_6F_5$ rings and the benzylic protons in these adducts in that rotation about the N−B and $N-C_{Bn}$ bonds may be to some extent "geared" by π-stacking interactions, as shown in Scheme 2. For example, this effect may partially rationalize why the barrier of 58.5(5) kJ mol^{-1} (20 °C) for exchange of the benzylic protons in **3-k**, which has two stacking interactions available, is higher than that found for the thermodynamic isomer **3-t** (52.1(5) kJ mol^{-1}, −10 °C) in which only one stacking interaction is possible. However, since adduct **4-t**, where the π-stacking interaction with the *N*-phenyl group is weaker, also exhibits a rigid structure (as evidenced by the 15 inequivalent ^{19}F nuclei), more standard steric factors must also be at play in restricting the rotation about the N−B and $N-C_{Bn}$ bonds. Still, these stacking interactions undoubtedly play a role in the solution structure and dynamic behavior of adducts **1**−**3**, in particular at low temperatures, and these effects may be important in directing the subsequent reactivity of the adducts with nucleophiles.

In summary, we have prepared a number of imine adducts of $B(C_6F_5)_3$ and found that, while kinetic

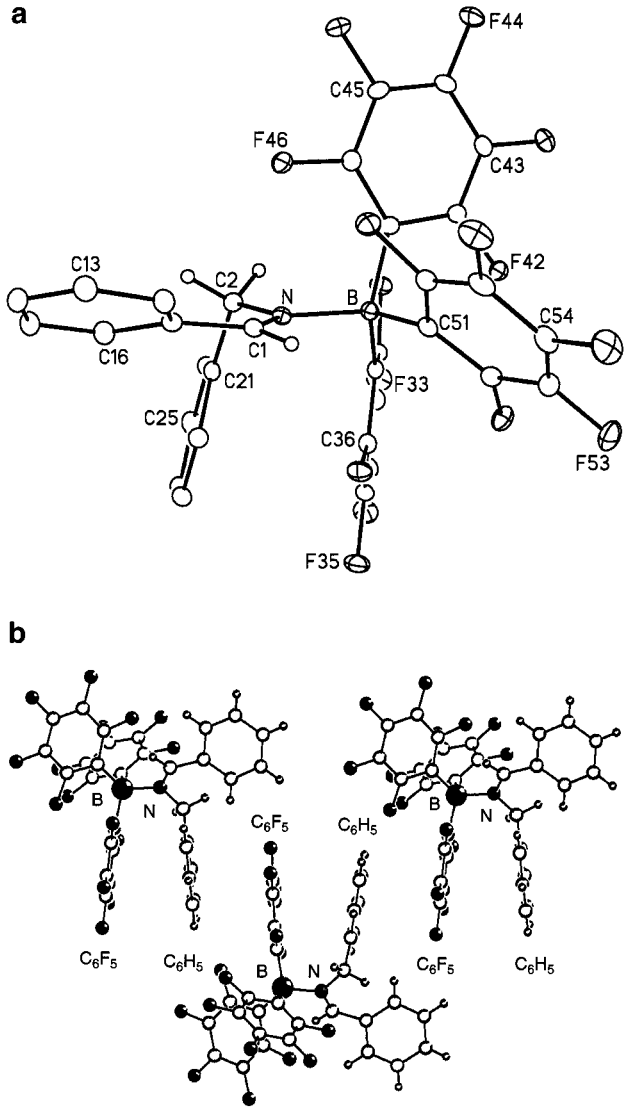

Figure 5. (a) ORTEP diagram of **3-t**. See Tables 1−3 for selected metrical parameters. (b) Partial crystal packing diagram for **3-t**, showing the intermolecular stacking arrangement.

adducts with the thermodynamically most stable geometric isomer of the free imine can be formed at low temperature, under conditions where the imines are labile the thermodynamic adduct (with the less stable geometric isomer of the imine) is readily formed. In cases where neither isomer of the free imine coordinates to the borane strongly, an adduct can be formed through the enamine tautomer (**5**) if α-protons are present. While these results suggest that the geometry of the adducts can be controlled in stoichiometric regimes, under conditions where borane is present in catalytic quantities, the speciation and reactivity of the imine−borane adducts will be governed by the complex interplay of the relevant rate constants.

Experimental Section

General Considerations. General procedures have been described in detail elsewhere.[8d] The imines used in this study were either purchased from Aldrich-Sigma and used as received or prepared via standard methodology. Aldimines were prepared by condensing the aldehyde and amine in CH_2Cl_2 followed by purification by recrystallization or distillation;

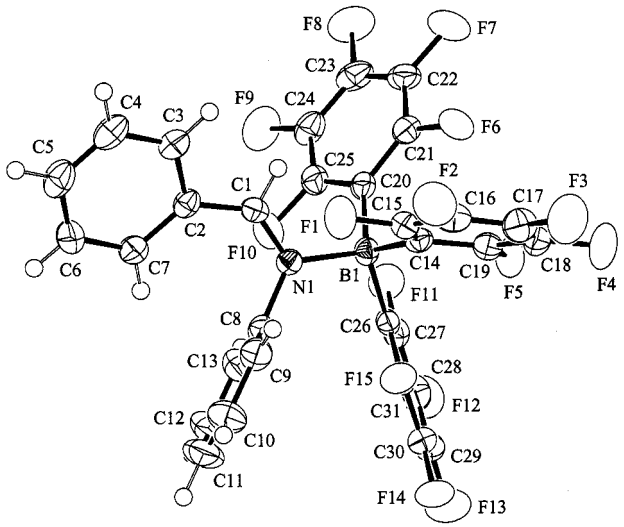

Figure 6. ORTEP diagram of **4-t**. See Tables 1−3 for selected metrical parameters.

ketimines were synthesized by mixing the ketone and amine in toluene and heating to reflux using a Dean−Stark apparatus in the presence of catalytic $ZnCl_2$, followed by purification.

Synthesis of $Ph_2C{=}N(Bn){\cdot}B(C_6F_5)_3$ (1). Crystals of adduct **1** suitable for X-ray crystallography and elemental analysis were obtained by mixing $B(C_6F_5)_3$ (51 mg, 0.10 mmol) and $Ph_2C{=}NPh$ (30 mg, 0.11 mmol) in toluene (approximately 0.5 mL) in a 1 dram vial. Hexane was added until the mixture became cloudy, and then the mixture was heated until all of the precipitate dissolved. The mixture was cooled to room temperature, over which time colorless crystals formed (yields ranging from 50 to 90%) from the first crystallization. NMR spectral characterization was carried out by mixing 1:1 ratio (0.1 mmol) of **1** and $Ph_2C{=}NPh$ in C_7D_8. ^{1}H NMR (C_7D_8, −40 °C): 7.89 (t, 1H, J = 9.2 Hz), 7.75 (br s, 1H), 6.95−6.24 (m, 13H), 5.79 (d, 1H, J = 15.6 Hz), 4.87 (d, 1H, J = 15.6 Hz); ^{1}H NMR (C_7D_8, 300 MHz, 25 °C; δ): 8.20−6.24 (m, 15H), 5.79 (br s, 1H), 4.98 (br s, 1H). ^{13}C NMR (C_6D_6, 100 MHz, −40 °C; δ): 190.2 (C=N), 139.4, 138.2, 136.3, 136.2, 133.8, 132.0, 131.7, 131.1, 129.3, 128.4, 128.1, 128.0, 127.4, 127.2, 126.9, 126.0, 125.4, 124.4, 61.1 (d), 21.8. ^{19}F NMR (C_7D_8, 282 MHz, −40 °C; δ): −119.5 (app t, 1F, *o*-F), −123.6 (app t, 1F, *o*-F), −129.0 (d, 1F, *o*-F), −131.4 (d, 1F, *o*-F), −132.5 (app t, 1F, *o*-F), −137.0 (app t, 1F, *o*-F), −155.6 (app t, 1F, *p*-F), −156.4 (app t, 1F, *p*-F), −156.8 (app. t, 1F, *p*-F), −162 to −163 (m, 4F, *m*-F's), −163.8 (app t, 1F, *m*-F), −164.2 (app t, 1F, *m*-F). ^{11}B NMR (C_7D_8, 64.18 MHz, 25 °C; δ): −3.7. IR (KBr, cm^{-1}): 1646 (C=N), 1573, 1513, 1470, 1282, 1088, 972, 796, 698. Anal. Calcd for $C_{38}H_{17}NBF_{15}$: C, 58.26; H, 2.19; N, 1.79. Found: C, 58.17; H, 2.28; N, 1.75.

Characterization of (*E*)-$Ph(CH_3)C{=}N(Bn){\cdot}B(C_6F_5)_3$ (2-k). Crystals of adduct **2-k** were obtained while attempting to isolate the thermodynamic isomer **2-t**. tThe imine $Ph(CH_3)C{=}NBn$ and $B(C_6F_5)_3$ were mixed in a 1:1 ratio (0.10 mmol) in toluene. A white precipitate formed that was dissolved by heating gently; the solution was cooled slowly to room temperature. X-ray-quality crystals deposited from this mixture, which contained both **2-k** and **2-t**, although visually different crystals were not distinguished in this sample. The crystal structure obtained was of the kinetic isomer **2-k**. To characterize **2-k** by NMR spectroscopy, the adduct was generated at low temperature by adding a solution of $B(C_6F_5)_3$ in C_7D_8 to $Ph(CH_3)C{=}NBn$ dissolved in C_7D_8 in an NMR tube cooled to −78 °C. ^{1}H NMR (C_7D_8, 400 MHz, −20 °C; δ): 7.38 (t, 1H), 6.89 (t, 1H), 6.82−6.76 (m, 3H), 6.71 (t, 1H), 6.52 (br s, 1H), 6.34−6.22 (m, 3H), 4.69 (br s, 2H, CH_2), 1.51 (s, 3H, CH_3). ^{19}F NMR (C_7D_8, 282 MHz, −40 °C; δ): −118.1 (br t, 1F, *o*-F), −124.4 (t, 1F, *o*-F), −129.3 (d, 1F, *o*-F), −133.0 (m, 2F, *o*-F's),

Scheme 2

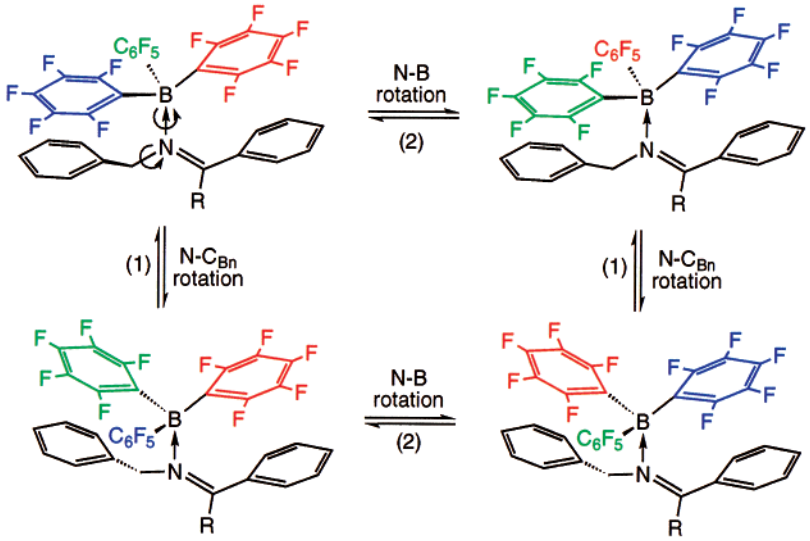

−139.6 (s, 1F, *o*-F), −155.9 (t, 1F, *p*-F), −156.1 (t, 1F, *p*-F), −156.9 (t, 1F, *p*-F), −162.4 to −163.2 (m, 4F, *m*-F's), −164.1 to −164.6 (m, 2F, *m*-F's). ^{13}C NMR analysis was precluded by the propensity of **2-k** to precipitate over longer periods of time in C_7D_8, CD_2Cl_2, and other solvents. The infrared spectrum and elemental analysis were obtained on the solid that immediately precipitates when $B(C_6F_5)_3$ and $Ph(CH_3)C{=}NBn$ are mixed at low temperature. IR (KBr, cm^{-1}): 1639 (C=N), 1601, 1515, 1459, 1278, 1088, 979, 760, 698, 504. Anal. Calcd for $C_{33}H_{15}NBF_{15}$: C, 54.95; H, 2.10; N, 1.94. Found: C, 54.54; H 2.05; N, 1.94.

Synthesis of (*Z*)-Ph(CH$_3$)C=N(Bn)·B(C$_6$F$_5$)$_3$ (2-t). A thermodynamic mixture of **2-t** and **2-k** (10:1) was prepared by mixing $Ph(CH_3)C{=}NBn$ and $B(C_6F_5)_3$ in C_7D_8 followed by heating to redissolve the precipiate that initially forms. Complete NMR spectral characterization was carried out. ^{1}H NMR of **2-t** (300 MHz, −40 °C; *δ*): 7.25−6.35 (m, 8H), 6.08 (m, 2H), 5.27 (d, 1H, *J* = 16.9 Hz), 5.02 (d, 1H, *J* = 16.9 Hz), 1.94 (s, 3H). ^{1}H NMR (300 MHz, 25 °C; *δ*): 6.83−6.52 (m, 8H), 6.16 (m, 2H), 5.23 (d, 1H, *J* = 16.4 Hz), 5.03 (d, 1H, *J* = 16.4 Hz), 2.09 (br s, 3H). ^{19}F NMR (282 MHz, −40 °C; *δ*): −129.8 (br s, 2F, *o*-F's), −130.2 (d, 1F, *o*-F), −130.5 (d, 1F, *o*-F), −132.7 (br s, 2F, *o*-F's), −155.0 (app t, 1F, *p*-F), −155.2 (app t, 1F, *p*-F), −155.4 (app t, 1F, *p*-F), −160.8 (app t, 1F, *m*-F), −161.4 (app t, 1F, *m*-F), −162.2 (app t, 1F, *m*-F), −162.6 (m, 1F, *m*-F), −162.9 (m, 1F, *m*-F), −163.4 (app t, 1F, *m*-F) (plus minor resonances for **t**−**k**). ^{13}C NMR (C_6D_6, 100 MHz, 25 °C; *δ*): 191.82 (*C*=N), 138.31, 135.14, 130.30, 128.76, 128.05, 127.15, 125.48, 124.82, 60.55 (m, *C*H$_2$), 28.94 (m, *C*H$_3$). ^{11}B NMR (128.34 MHz, 25 °C; *δ*): −4.7. Crystals of **2-t** were obtained from the 10:1 mixture of **2-t** and **2-k** (0.10 mmol) dissolved in C_7D_8 in an NMR tube (62% recovery). IR (KBr, cm^{-1}): 1651 (C=N), 1596, 1519, 1454 (br), 1372, 1279, 1105 (br), 968. Anal. Calcd for $C_{33}H_{15}NBF_{15}$: C, 54.95; H, 2.10; N, 1.94. Found: C, 54.51; H, 1.93; N, 1.99%. These IR spectral and analytical data were obtained on crystalline material obtained under thermodynamic conditions.

Characterization of (*E*)-Ph(H)C=N(Bn)·B(C$_6$F$_5$)$_3$ (3-k). The adduct **3-k** was generated at low temperature by adding a solution of $B(C_6F_5)_3$ (26 mg, 0.05 mmol) to the aldimine (9 mg, 0.05 mmol) dissolved in C_7D_8 in an NMR tube at low temperature. ^{1}H and ^{19}F NMR spectra could be obtained, but a ^{13}C NMR spectrum was not obtained, since **3-k** precipitates in the NMR tube soon after it is formed. Warming the reaction mixture to room temperature leads to conversion of adduct **3-k** to adduct **3-t**. ^{1}H NMR (C_7D_8, 300 MHz, −40 °C; *δ*): 7.69 (s, 1H), 7.04 (d, 2H, *J* = 9.8 Hz), 6.86−6.66 (m, 4H), 6.54 (t, 2H, *J* = 8.5 Hz), 6.32 (d, 2H, *J* = 6.9 Hz), 4.68 (d, 1H, *J* = 14.9 Hz), 4.31 (d, 1H, *J* = 14.9 Hz). ^{19}F NMR (C_7D_8, 282 MHz, −40 °C; *δ*): −121.1 (br s, 1F, *o*-F), −122.6 (app t, 1F, *o*-F), −124.3 (d, 1F, *o*-F), −127.0 (br s, 1F, *o*-F), −127.9 (d, 1F, *o*-F), −132.0 (br s, 1F, *o*-F), −150.7 (app t, 2F, *p*-F), −150.9 (app t, 1F, *p*-F), −157.0 (app td, 1F, *m*-F), −157.5 (app td, 1F, *m*-F), −158.0 (app td, 1F, *m*-F), −158.3 (app td, 1F, *m*-F), −159.2 (app td, 1F, *m*-F), −159.5 (app td, 1F, *m*-F). ^{11}B NMR (C_6D_6, 64.18 MHz, 25 °C; *δ*): −6.6. Infrared spectral and analytical data were obtained on precipitate formed at low temperature. IR (KBr, cm^{-1}): 1651 (C=N), 1531, 1383, 1290, 1115 (br), 963 (br), 793. Anal. Calcd for $C_{33}H_{13}NBF_{15}$: C, 54.34; H, 1.85; N, 1.98. Found: C, 54.84; H, 2.00; N, 1.89.

Synthesis of (*Z*)-Ph(H)C=N(Bn)·B(C$_6$F$_5$)$_3$ (3-t). Colorless crystals of **3-t** were obtained by dissolving a 1:1 mixture of $B(C_6F_5)_3$ and $Ph(H)C{=}NBn$ (0.1 mmol) in toluene, adding hexane until cloudy, heating to dissolution, and then standing at room temperature (77% recovery). ^{1}H NMR (300 MHz, −40 °C; *δ*): 8.68 (d, 1H, *J* = 7.2 Hz, C*H*=N), 7.05 (brs, 2H), 6.79 (t, 1H, *J* = 7.4 Hz), 6.70−6.63 (m, 3H), 6.57 (t, 2H, *J* = 7.4 Hz), 6.35 (m, 2H), 5.25 (d, 1H, *J* = 15.6 Hz), 4.87 (d, 1H, *J* = 15.6 Hz). ^{19}F NMR (282 MHz, −40 °C; *δ*): −129.0 (m, 2F, *o*-F's), −129.2 (br s, 1F, *o*-F), −131.2 (d, 1F, *o*-F), −134.2 (d, 1F, *o*-F), −136.3 (app t, 1F, *o*-F), −153.5 (app t, 1F, *p*-F), −155.9 (app t, 1F, *p*-F), −156.0 (app t, 1F, *p*-F), −159.8 (app td, 1F, *m*-F), −161.8 − −162.3 (m, 2F, *m*-F's), −162.5 − −162.8 (m, 2F, *m*-F's), −163.9 (m, 1F, *m*-F). ^{13}C NMR ($CDCl_3$, 100 MHz, −40 °C; *δ*): 171.0 (*C*=N), 135.6, 132.8, 132.4, 130.2, 128.6, 128.4, 127.8, 125.3, 56.2 (d, *C*H$_2$) (broad resonances from $B(C_6F_5)_3$ not included). ^{11}B NMR (C_7D_8, 64.18 MHz, 25 °C; *δ*): −3.3. Anal. Calcd for $C_{32}H_{12}NBF_{15}$: C, 54.34; H, 1.85; N, 1.98. Found: C, 54.19; H, 1.58; N, 1.98. Infrared spectral and analytical data were obtained on crystalline material obtained under thermodynamic conditions.

Characterization of Ph(H)C=N(Ph)·B(C$_6$F$_5$)$_3$ (4-t). An NMR tube was charged with Ph(H)C=NPh (18 mg, 0.10 mmol), $B(C_6F_5)_3$ (51 mg, 0.10 mmol), and C_7D_8. NMR spectra of this compound were measured. ^{1}H NMR (C_7D_8, 300 MHz, 25 °C; *δ*): 7.89 (s, 1H, C(*H*)=N), 7.20−6.50 (m, 10H). ^{13}C NMR (C_6D_6, 25 °C; *δ*): 174.76, 151.03, 143.11, 135.28, 134.61, 133.14, 131.47, 130.02, 129.90, 129.79, 129.57, 129.41, 125.81. ^{19}F NMR (C_7D_8, 282 MHz, −20 °C; *δ*): −122.1 (d, 1F, *o*-F), −126.1 (d, 1F, *o*-F), −126.9 (d, 1F, *o*-F), −132.4 (s, 1F, *o*-F), −133.8 (d, 1F, *o*-F), −138.6 (d, 1F, *o*-F), −155.0 (app t, 1F, *p*-F), −155.7 (app t, 1F, *p*-F), −155.9 (app t, 1F, *p*-F), −162.4 (m, 1F, *m*-F), −162.9 (m, 1F, *m*-F), −163.4 to −163.7 (m, 2F, *m*-F's), −164.9 (m, 1F, *m*-F), −165.1 (m, 1F, *m*-F). Crystals suitable for X-ray analysis were obtained from the NMR tube. IR spectral and analytical data were obtained on this crystalline material. IR

Table 4. Summary of Data Collection and Structure Refinement Details for Imine Adducts of $B(C_6F_5)_3$.

	1	2-k	2-t	3-t	4-t	5
formula	$C_{38}H_{17}BNF_{15}\cdot 0.5C_8H_7$	$C_{33}H_{15}BNF_{15}\cdot 0.5C_7H_8$	$C_{33}H_{15}BNF_{15}$	$C_{32}H_{13}BNF_{15}$	$C_{31}H_{11}BNF_{15}$	$C_{31}H_{19}BNF_{15}$
fw	829.42	767.34	721.27	707.24	693.22	701.28
cryst syst	triclinic	monoclinic	triclinic	monoclinic	triclinic	monoclinic
a, Å	12.706(5)	22.036(2)	9.6120(3)	14.144(4)	9.983(3)	16.530(2)
b, Å	13.574(7)	15.833(1)	11.4664(4)	13.679(4)	17.673(4)	9.8869(9)
c, Å	11.860(8)	20.376(1)	13.4295(4)	15.863(5)	8.184(2)	18.070(2)
α, deg	113.10(4)	79.983(2)	101.71(2)			
β, deg	101.03(5)	115.582(1)	88.101(2)	115.267(6)	104.60(2)	104.153(2)
γ, deg	96.88(5)	81.833(1)	86.36(2)			
V, Å^3	1803.3(20)	6412.0(8)	1442.73(8)	2775.2(14)	1368.1(6)	2863.5(4)
space group	$P\bar{1}$	$P2_1/c$	$P\bar{1}$	$P2_1/n$	$P\bar{1}$	$P2_1/n$
Z	2	8	2	4	2	4
d_{calcd}, mg m^{-3}	1.527	1.590	1.660	1.693	1.683	1.627
μ, mm^{-1}	0.143	0.154	0.17	0.169	0.163	0.163
no. of rflns	6699	32 358	11 944	13 490	5148	14 351
no. of unique rflns	6387	12 952	6465	5741	4853	5877
no. of variables	541	957	451	442	434	433
R	0.040				0.040	
R_w	0.040				0.041	
R1		0.0765	0.046	0.0371		0.0340
wR2		0.1457	0.118	0.0870		0.0908
GOF	1.40	0.939	1.02	0.904	2.79	1.031

(KBr, cm^{-1}): 1667 (C═N), 1651, 1596, 1520, 1088, 766. Anal. Calcd for $C_{31}H_{11}NBF_{15}$: C, 53.45; H, 1.60; N, 2.02. Found: C, 53.71; H, 1.43; N, 2.06.

Synthesis of Zwitterion 5. Colorless crystals of **5** were obtained in 44% yield by mixing $B(C_6F_5)_3$ and $^tBu(CH_3)C$═NBn in a 1:1 ratio (0.1 mmol each) in toluene at room temperature followed by cooling to −30 °C. Characterization of **5** in solution was achieved by mixing $B(C_6F_5)_3$ and $^tBu(CH_3)C$═NBn in a 4:1 ratio, under which conditions **5** predominates. ^{1}H NMR (400 MHz, C_6D_6; *δ*): 7.07 (br s, 1H, N*H*), 7.00−6.80 (m, 3H), 6.36 (d, 2H, *J* = 6.9 Hz), 3.40 (br s, 2H, CH_2B), 3.30 (d, 2H, *J* = 5.7 Hz, NCH_2Ph), 0.36 (s, 9H). ^{13}C NMR (100 MHz, C_6D_6; *δ*): 212.87 (*C*═N), 132.39, 130.07, 130.00, 127.58, 50.60, 42.99, 42.95 (*C*$(CH_3)_3$), 27.07 (*C*H_3). ^{19}F NMR (282 MHz, C_6D_6; *δ*): −131.41 (br s, 2F, *o*-F), −158.88 (br s, 1F, *p*-F), −164.24 (brs, 2F, *m*-F). ^{11}B NMR (128.4 MHz, C_6D_6; *δ*): −12.2. Infrared spectral and analytical data were obtained on crystalline **5** that had been crushed into a powder. IR (KBr, cm^{-1}): 3632 (w), 3540 (w), 3356 (s, NH), 2972, 1644 (C═N), 1618, 1516, 1454, 1368, 1270, 1148, 1081, 974, 862, 754, 688. Anal. Calcd for $C_{31}H_{19}NBF_{15}$: C, 53.09; H, 2.73; N, 2.00. Found: C, 53.09; H, 2.20; N, 1.96.

X-ray Crystallography. A summary of crystal data and refinement details for all structures is given in Table 4. Suitable crystals were covered in Paratone oil, mounted on a glass fiber, and immediately placed in a cold stream on the diffractometer employed.

1 and 4-t. Crystals of **1** and **4-t** were grown from a toluene solution. Measurements were made using a Rigaku AFC6S diffractometer with a graphite-monochromated Mo Kα radiation (λ = 0.710 69 Å) source at −103 °C with the $\omega-2\theta$ scan technique to a maximum 2θ value of 50.1°. The structure was solved by direct methods and expanded using Fourier techniques. The non-hydrogen atoms were refined anisotropically; hydrogen atoms were included at geometrically idealized positions with C−H = 0.95 Å and were not refined. All calculations were performed using the teXsan crystallographic software package of Molecular Structure Corp.[21]

2-t. Crystals of **2-t** were grown from a toluene solution. Measurements were made using a Nonius KappaCCD diffractometer with graphite-monochromated Mo Kα radiation (λ = 0.710 73 Å). Cell constants obtained from the refinement of 6086 reflections in the range $1.0 < \theta < 27.5°$ corresponded to a primitive triclinic cell. The data were collected at 170(2) K using the $\omega-\varphi$ scans to a maximum θ value of 27.5°. The structure was solved by direct methods and expanded using Fourier techniques. The non-hydrogen atoms were refined anisotropically; hydrogen atoms were included at geometrically idealized positions with C−H = 0.95 Å and were not refined. All calculations were performed using SHELXTL97.[22]

2-k, 3-t, 5. Colorless crystals were obtained from toluene (**2-k**), toluene/hexanes (**3-t**), or C_6D_6 (**5**). Data were collected on a Bruker P4/RA/SMART 1000 CCD diffractometer[23] using Mo Kα radiation at −80 °C. Unit cell parameters were obtained from a least-squares refinement of the setting angles of 4839 reflections from the data collection. An empirical absorption correction was applied to the data through use of the SADABS procedure. The structures were solved using the direct methods program SHELXS-86,[24] and full-matrix least-squares refinement on F^2 was completed using the program SHELXL-93.[25] Hydrogen atoms were assigned positions based on the geometries of their attached carbon atoms and were given isotropic thermal parameters 20% greater than the equivalent isotropic displacement parameters of the attached carbons. For **2-k**, along with one molecule of cocrystallized toluene, the asymmetric unit was found to contain two crystallographically independent molecules of **2-k**, which showed no significant differences in bond lengths, bond angles, or conformational angles.

Acknowledgment. Funding for this work came from the Natural Sciences and Engineering Research Council of Canada in the form of a Research Grant (to W.E.P.), an E. W. R. Steacie Fellowship (2001−2003; to W.E.P.) and Scholarship support (PGSB; to J.M.B.). J.M.B. also thanks the Killam Foundation for a Fellowship and the Alberta Heritage Foundation for a Steinhauer Award. Mr. Eric Sonmor is thanked for preliminary experiments and technical support at an early stage of the project.

Supporting Information Available: Full listings of crystallographic data, atomic parameters, hydrogen parameters, atomic coordinates, and complete bond distances and angles for **1**, **2-k**, **2-t**, **3-t**, **4-t**, and **5**. This material is available free of charge via the Internet at http://pubs.acs.org.

OM011086N

(21) teXan: Crystal Structure Analysis Package; Molecular Structure Corp., 1985, 1992.

(22) Sheldrick, G. M., SHELXTL97: Program for Crystal Structure Determination; University of Göttingen, Göttingen, Germany, 1997.

(23) Programs for diffractometer operation, data collection, data reduction, and absorption correction were those supplied by Bruker.

(24) Sheldrick, G. M. *Acta Crystallogr.* **1990**, *A46*, 467−473.

(25) Sheldrick, G. M. SHELXL-93: Program for Crystal Structure Determination; University of Göttingen, Göttingen, Germany, 1993.